Calibration and Analysis of the GCT Camera for the Cherenkov Telescope Array

Jason J. Watson

Brasenose College
University of Oxford

A thesis submitted for the degree of
Doctor of Philosophy

Trinity 2018

Abstract

Lorem ipsum dolor sit amet, consectetur adipiscing elit. Pellentesque sit amet nibh volutpat, scelerisque nibh a, vehicula neque. Integer placerat nulla massa, et vestibulum velit dignissim id. Ut eget nisi elementum, consectetur nibh in, condimentum velit. Quisque sodales dui ut tempus mattis. Duis malesuada arcu at ligula egestas egestas. Phasellus interdum odio at sapien fringilla scelerisque. Mauris sagittis eleifend sapien, sit amet laoreet felis mollis quis. Pellentesque dui ante, finibus eget blandit sit amet, tincidunt eu neque. Vivamus rutrum dapibus ligula, ut imperdiet lectus tincidunt ac. Pellentesque ac lorem sed diam egestas lobortis.

Suspendisse leo purus, efficitur mattis urna a, maximus molestie nisl. Aenean porta semper tortor a vestibulum. Suspendisse viverra facilisis lorem, non pretium erat lacinia a. Vestibulum tempus, quam vitae placerat porta, magna risus euismod purus, in viverra lorem dui at metus. Sed ac sollicitudin nunc. In maximus ipsum nunc, placerat maximus tortor gravida varius. Suspendisse pretium, lorem at porttitor rhoncus, nulla urna condimentum tortor, sed suscipit nisi metus ac risus.

Aenean sit amet enim quis lorem tristique commodo vitae ut lorem. Duis vel tincidunt lacus. Sed massa velit, lacinia sed posuere vitae, malesuada vel ante. Praesent a rhoncus leo. Etiam sed rutrum enim. Pellentesque lobortis elementum augue, at suscipit justo malesuada at. Lorem ipsum dolor sit amet, consectetur adipiscing elit. Praesent rhoncus convallis ex. Etiam commodo nunc ex, non consequat diam consectetur ut. Pellentesque vitae est nec enim interdum dapibus. Donec dapibus purus ipsum, eget tincidunt ex gravida eget. Donec luctus nisi eu fringilla mollis. Donec eget lobortis diam.

Suspendisse finibus placerat dolor. Etiam ornare elementum ex ut vehicula. Donec accumsan mattis erat. Quisque cursus fringilla diam, eget placerat neque bibendum eu. Ut faucibus dui vitae dolor porta, at elementum ipsum semper. Sed ultrices dui non arcu pellentesque placerat. Etiam posuere malesuada turpis, nec malesuada tellus malesuada.

Calibration and Analysis of the GCT Camera for the Cherenkov Telescope Array

Jason J. Watson

Brasenose College

University of Oxford

A thesis submitted for the degree of

Doctor of Philosophy

Trinity 2018

Acknowledgements

Personal

Lorem ipsum dolor sit amet, consectetur adipiscing elit. Vestibulum feugiat et est at accumsan. Praesent sed elit mattis, congue mi sed, porta ipsum. In non ullamcorper lacus. Quisque volutpat tempus ligula ac ultricies. Nam sed erat feugiat, elementum dolor sed, elementum neque. Aliquam eu iaculis est, a sollicitudin augue. Cras id lorem vel purus posuere tempor. Proin tincidunt, sapien non dictum aliquam, ex odio ornare mauris, ultrices viverra nisi magna in lacus. Fusce aliquet molestie massa, ut fringilla purus rutrum consectetur. Nam non nunc tincidunt, rutrum dui sit amet, ornare nunc. Donec cursus tortor vel odio molestie dignissim. Vivamus id mi erat. Duis porttitor diam tempor rutrum porttitor. Lorem ipsum dolor sit amet, consectetur adipiscing elit. Sed condimentum venenatis consectetur. Lorem ipsum dolor sit amet, consectetur adipiscing elit.

Aenean sit amet lectus nec tellus viverra ultrices vitae commodo nunc. Mauris at maximus arcu. Aliquam varius congue orci et ultrices. In non ipsum vel est scelerisque efficitur in at augue. Nullam rhoncus orci velit. Duis ultricies accumsan feugiat. Etiam consectetur ornare velit et eleifend.

Suspendisse sed enim lacinia, pharetra neque ac, ultricies urna. Phasellus sit amet cursus purus. Quisque non odio libero. Etiam iaculis odio a ex volutpat, eget pulvinar augue mollis. Mauris nibh lorem, mollis quis semper quis, consequat nec metus. Etiam dolor mi, cursus a ipsum aliquam, eleifend venenatis ipsum. Maecenas tempus, nibh eget scelerisque feugiat, leo nibh lobortis diam, id laoreet purus dolor eu mauris. Pellentesque habitant morbi tristique senectus et netus et malesuada fames ac turpis egestas. Nulla eget tortor eu arcu sagittis euismod fermentum id neque. In sit amet justo ligula. Donec rutrum ex a aliquet egestas.

Institutional

Lorem ipsum dolor sit amet, consectetur adipiscing elit. Ut luctus tempor ex at pretium. Sed varius, mauris at dapibus lobortis, elit purus tempor neque, facilisis sollicitudin felis nunc a urna. Morbi mattis ante non augue blandit pulvinar. Quisque nec euismod mauris. Nulla et tellus eu nibh auctor malesuada quis imperdiet quam. Sed eget tincidunt velit. Cras molestie sem ipsum, at faucibus quam mattis vel. Quisque vel placerat orci, id tempor urna. Vivamus mollis, neque in aliquam consequat, dui sem volutpat lorem, sit amet tempor ipsum felis eget ante. Integer lacinia nulla vitae felis vulputate, at tincidunt ligula maximus. Aenean

venenatis dolor ante, euismod ultrices nibh mollis ac. Ut malesuada aliquam urna, ac interdum magna malesuada posuere.

CTA

ctapipe, target, chec.....

Abstract

Lorem ipsum dolor sit amet, consectetur adipiscing elit. Pellentesque sit amet nibh volutpat, scelerisque nibh a, vehicula neque. Integer placerat nulla massa, et vestibulum velit dignissim id. Ut eget nisi elementum, consectetur nibh in, condimentum velit. Quisque sodales dui ut tempus mattis. Duis malesuada arcu at ligula egestas egestas. Phasellus interdum odio at sapien fringilla scelerisque. Mauris sagittis eleifend sapien, sit amet laoreet felis mollis quis. Pellentesque dui ante, finibus eget blandit sit amet, tincidunt eu neque. Vivamus rutrum dapibus ligula, ut imperdiet lectus tincidunt ac. Pellentesque ac lorem sed diam egestas lobortis.

Suspendisse leo purus, efficitur mattis urna a, maximus molestie nisl. Aenean porta semper tortor a vestibulum. Suspendisse viverra facilisis lorem, non pretium erat lacinia a. Vestibulum tempus, quam vitae placerat porta, magna risus euismod purus, in viverra lorem dui at metus. Sed ac sollicitudin nunc. In maximus ipsum nunc, placerat maximus tortor gravida varius. Suspendisse pretium, lorem at porttitor rhoncus, nulla urna condimentum tortor, sed suscipit nisi metus ac risus.

Aenean sit amet enim quis lorem tristique commodo vitae ut lorem. Duis vel tincidunt lacus. Sed massa velit, lacinia sed posuere vitae, malesuada vel ante. Praesent a rhoncus leo. Etiam sed rutrum enim. Pellentesque lobortis elementum augue, at suscipit justo malesuada at. Lorem ipsum dolor sit amet, consectetur adipiscing elit. Praesent rhoncus convallis ex. Etiam commodo nunc ex, non consequat diam consectetur ut. Pellentesque vitae est nec enim interdum dapibus. Donec dapibus purus ipsum, eget tincidunt ex gravida eget. Donec luctus nisi eu fringilla mollis. Donec eget lobortis diam.

Suspendisse finibus placerat dolor. Etiam ornare elementum ex ut vehicula. Donec accumsan mattis erat. Quisque cursus fringilla diam, eget placerat neque bibendum eu. Ut faucibus dui vitae dolor porta, at elementum ipsum semper. Sed ultrices dui non arcu pellentesque placerat. Etiam posuere malesuada turpis, nec malesuada tellus malesuada.

Contents

List of Figures

Abbreviations

CHEC Compact High Energy Camera.

DCR Dark-Count Rate.

GCT Gamma-ray Cherenkov Telescope.

MAPMT Multi-Anode Photomultiplier Tube.

NSB Night-Sky Background.

PDE Photon Detection Efficiency.

SiPM Silicon Photomultiplier.

SPE Single Photo-Electron.

1

The Compact High Energy Camera

Contents

:

1.1 Plan

1.1.1 Topics

- Introduce TARGET architecture & Wilkinson ADC
- Different TARGET versions
- FEE
- MAPMs
- SiPMS
  - How they work
  - Comparison investigations
  - Property trade-offs
- CHEC-M
- Changes for CHEC-S
- Future - MUSIC ASICs

1.1.2 Questions

- ?

:

- number of pixels
- number of modules
- number of pixels per module
- number of cells
- pixel gaps
- module gaps

1.2 Introduction

The camera that has been designed for Gamma-ray Cherenkov Telescope (GCT) is known as Compact High Energy Camera (CHEC)

Two designs have been implemented for CHEC: an Multi-Anode Photomultiplier Tube (MAPMT) based camera

1.3 CHEC-M

schematic illustration of electronics

1.3.1 Multi-Anode Photomultiplier Tubes

connection between gain and hv

table of parameters

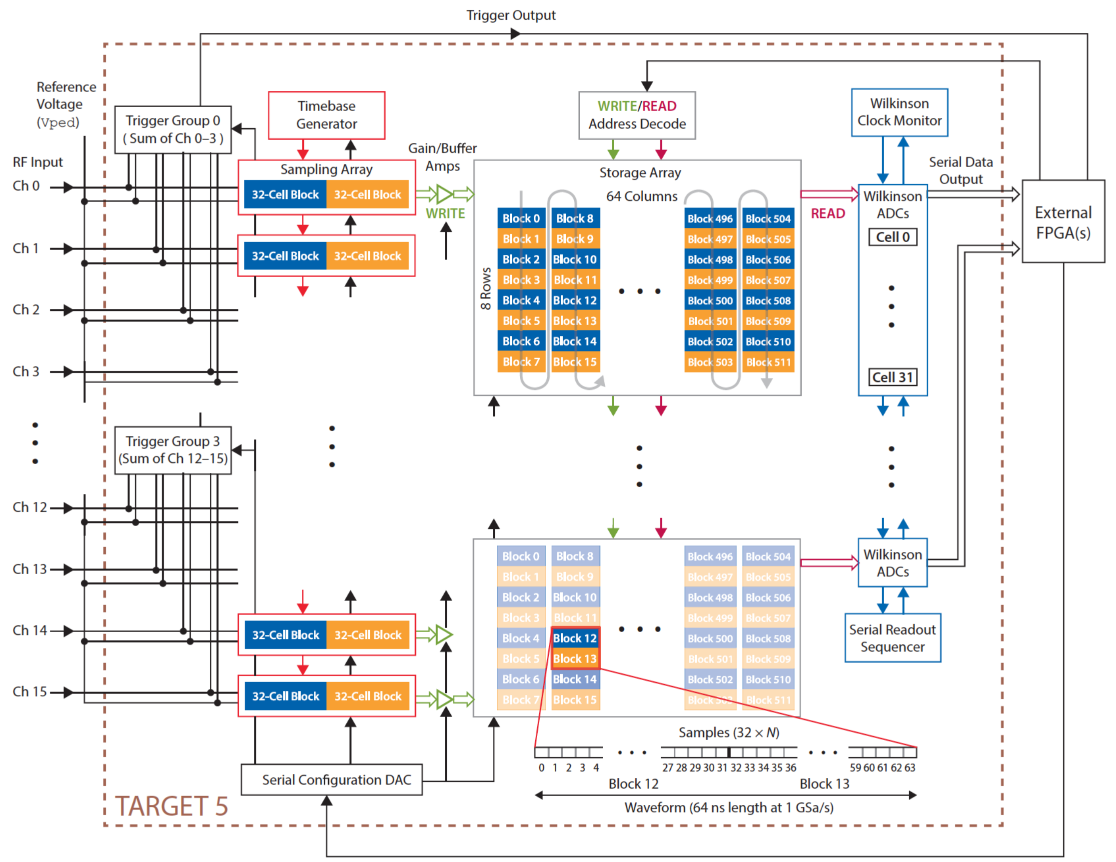

Figure 1.1: Functional block diagram of the TARGET 5 ASIC [1]

Add more details

1.3.2 Front-End Electronics

Pre-Amplifiers

TARGET

1.3.3 Back-End Electronics

Backplane

DACQ Boards

1.4 CHEC-S

1.4.1 Silicon Photomultipliers

connection between gain and bias voltage

table of parameters

1.4.2 TARGET-C

larger dynamic range, reference tf plot????

name of TARGET-C FPGA?

1.5 External Components

1.5.1 LED Flashers

1.5.2 Chiller

1.6 Future

1.7 Laboratory Set-Up

1.8 Laboratory Calibration

In order to obtain reliable knowledge on the average illumination incident on the camera in our laboratory, it was necessary to calibrate the laser and filter wheel combination. This was of paramount importance for performing the camera flat-field calibration, and for obtaining a laboratory charge resolution result. There exists three stages required to achieve a calibration from filter-wheel position to average expected charge in each pixel:

1. Measuring the relationship between filter-wheel position and light transmissivity.
2. Measuring the relative amount of light each pixel receives due to its position on the focal surface.
3. Measuring an absolute illumination in photoelectrons for at least one filter-wheel position.

Through combining the results of these stages, a conversion from filter-wheel position to expected number of photoelectrons in each pixel was obtained.

1.8.1 Filter Wheel

The calibration of the filter wheel was performed in two stages: an initial measurement with a reference Silicon Photomultiplier (SiPM) in order to obtain an approximate handle on the relative illumination, and a secondary correction using the camera at different gain settings.

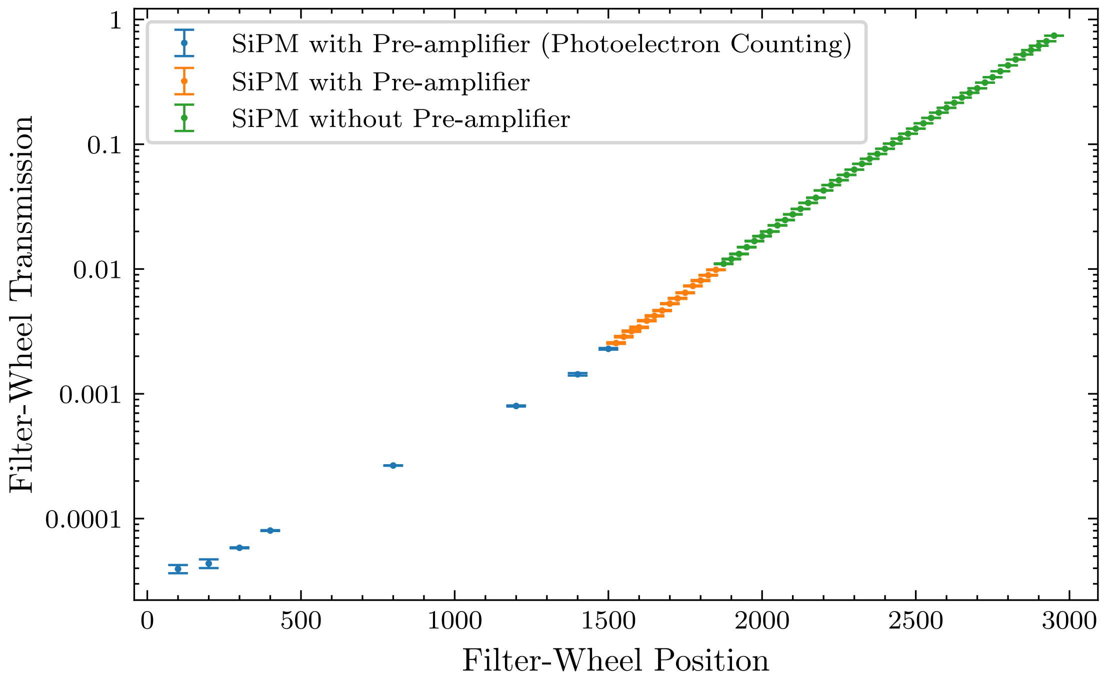

Figure 1.2: Logarithm of transmission versus position for the filter wheel. The relationship is fit with a straight line.

Reference SiPMT

Using a single reference silicon photomultiplier pixel connected to an oscilloscope, centred on the camera focal plane, the ratio between the signal with and without the neutral-density filter was calculated for different filter-wheel positions (i.e. different attenuations). As the dynamic range of the reference SiPM was limited, in order to cover the full range of filters attenuations, three approaches were utilised:

1. **Low-range** - Average illumination obtained from Single Photo-Electron (SPE) spectrum, with a pre-amplifier attached to the SiPM.
2. **Mid-range** - Average pulse area, with a pre-amplifier attached to the SiPM.
3. **High-range** - Average pulse area, with no pre-amplifier attached.

The overlapping values from each method were used to stitch the datasets together. The resulting points, shown in Figure 1.2, were then used as a lookup table for the conversion from filter-wheel position to transmission.

Camera Correction

When looking at the average measured charge across the camera as a function of transmission, for three datasets where each has different bias voltages applied

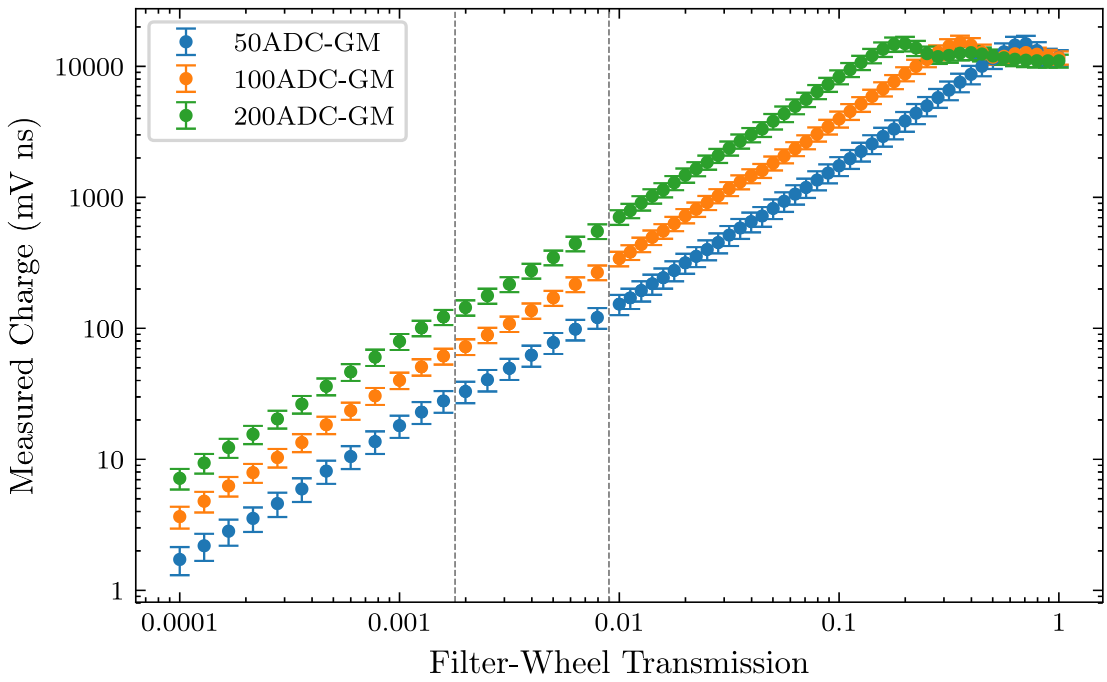

Figure 1.3: Average charge across all CHEC-S pixels versus filter-wheel transmission. Three differently-gain-matched datasets are shown (50 ADC, 100 ADC, 200 ADC). Each gain matching results in a different bias voltage across the photosensor, and therefore a different gain, optical crosstalk, and PDE. Features shared between the datasets at a transmission value can only be due to errors in the filter-wheel calibration. Two clear features are highlighted by the vertical grey lines. Features shared at a measured charge value are due to shared properties in the Transfer Function (such as saturation).

to the photosensors, features that share a position on the X axis can only occur from artefacts of the previous filter-wheel calibration. Figure 1.3 indicates some of the artefacts which are easy to see. The measured charge was then converted into an "effective transmission" using the relation in Figure 1.3. By plotting the "effective transmission" against filter-wheel position, a new conversion from filter-wheel position to transmission was obtained from the fit shown in Figure 1.4.

1.8.2 Illumination Profile

Two contributions influence the relative amount of light each pixel receives, depending on its position on the camera focal surface. The first is due to the laser uniformity characteristics, the second is due to the curved focal surface of the camera.

Laser Profile

Despite attempts to homogenise the illumination from the laser-diffuser combination, there are still non-uniformities in the light received at the camera pixels that needed

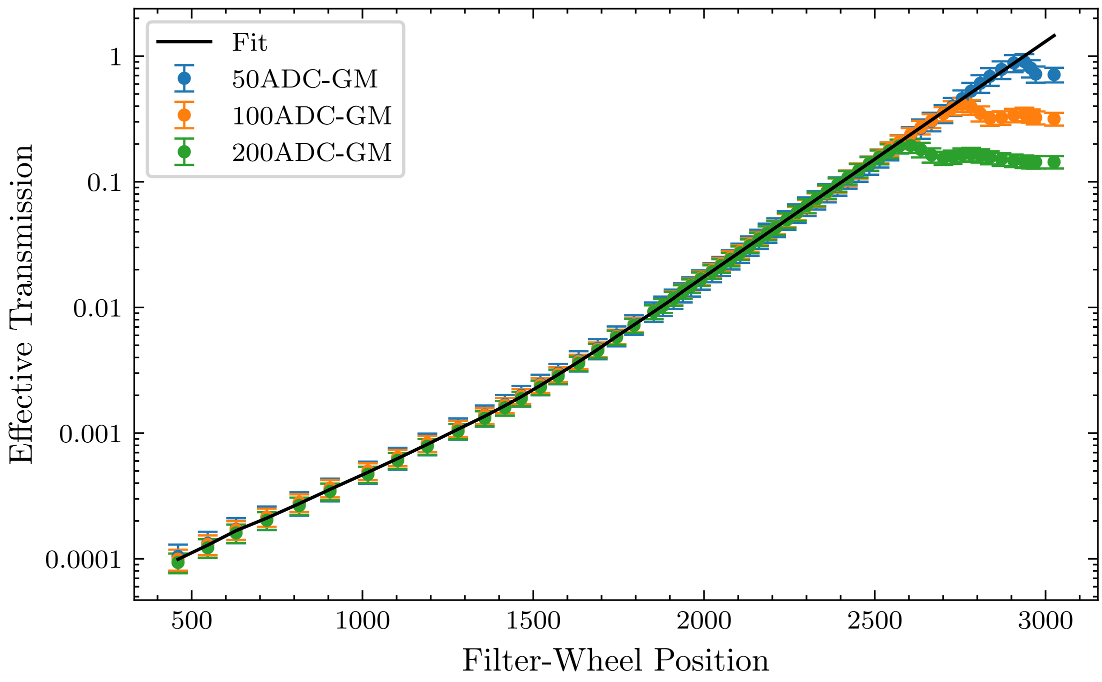

Figure 1.4: The measured charges from Figure 1.3 converted into an "effective transmission", providing a filter-wheel calibration that is corrected for artefacts resulting from the first stage of calibration.

Figure 1.5: Spatial profile of the laser illumination along a flat plane in front of the camera, measured with a single reference SiPM pixel attached to a robot arm.

Show value in each position, and then gradient fit?

.

to be accounted for in the calibration. As shown in Figure 1.5, a linear gradient in laser illumination exists across the x-y plane. This was found by attaching a single silicon photomultiplier pixel to a robot arm, and placing it at the camera position in from of the laser. Through the use of a single pixel, the amplitude measured is disentangled from the relative PDE. This pixel was then moved to each x-y position to calculate the ratio in signal amplitude, returning back to the origin to obtain a fresh value for comparison, thereby correcting for any deviations that may have occurred due to a change in temperature. The resulting distribution of ratios was fit with a linear gradient across the plane.

Camera Geometry

Talk about how this is an approximation - modules are fixed along focal plane, light-source is somewhat between pointlike and at infinity, quote percentage that difference makes

Add not to scale on figure

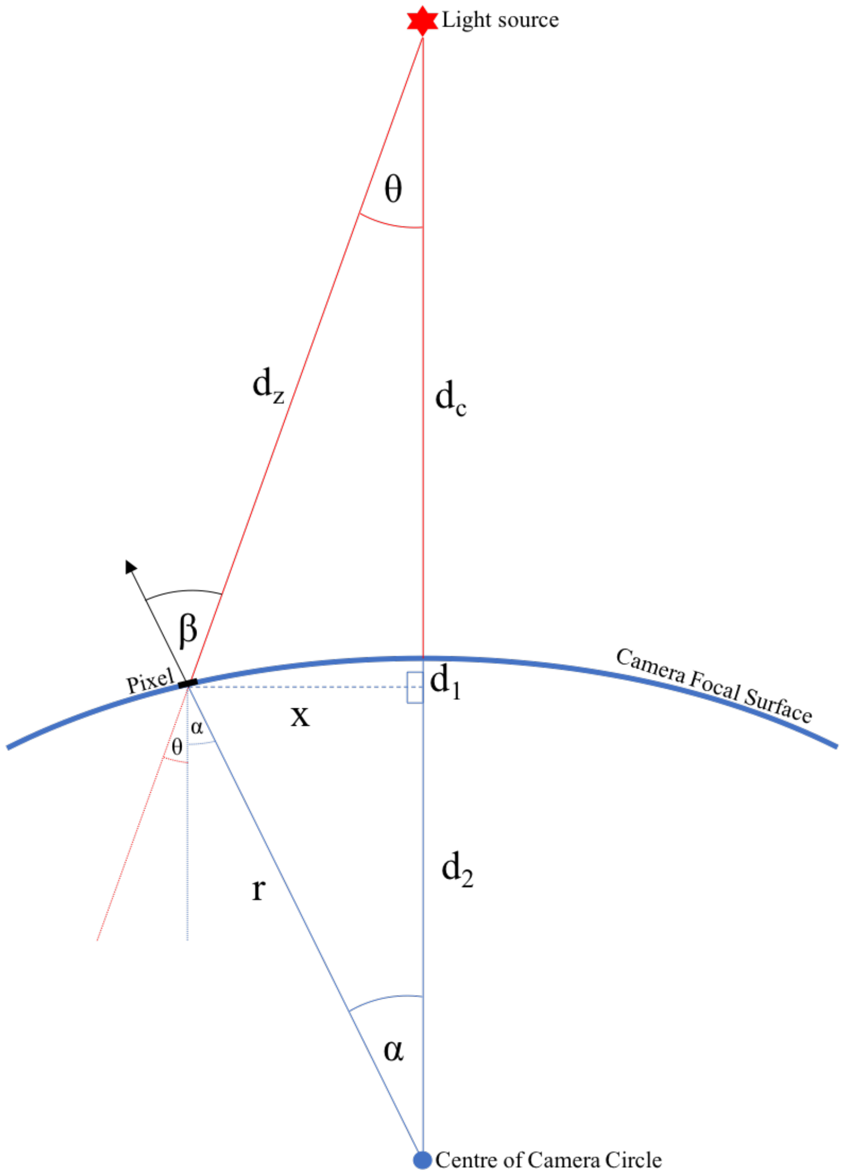

Figure 1.6: Two-dimensional geometry schematic of the laboratory set-up for uniform camera illumination, used to calculate the reduction in light level for each pixel depending on its distance from the camera centre.

Due to the spherical camera focal surface, each pixel is at a different distance d_z from the light-source, and therefore receives a different amount of light depending on its distance x from the camera centre. Furthermore, at a "viewing angle" β, i.e. the angle between the normal to the pixel and the light-source, the amount of surface area of the pixel A_P visible to the light-source is reduced. The visible surface area is known as the "viewing area" A_V. The combined geometric correction to the light intensity required to compensate for these effects is almost circularly symmetric, and therefore can be analytically approximated by using a two dimensional description of the camera, with a circular focal surface:

$$d_1 = r - d_2 = r - \sqrt{r^2 - x^2}, \tag{1.8.2.1}$$

$$d_z = \sqrt{x^2 + (d_c + d_1)^2} = \sqrt{x^2 + (d_c + r - \sqrt{r^2 - x^2})^2}. \tag{1.8.2.2}$$

$$\beta = \theta + \alpha = \sin^{-1}\frac{x}{d_z} + \sin^{-1}\frac{x}{r}, \tag{1.8.2.3}$$

$$\frac{A_V}{A_P} = \cos\beta, \tag{1.8.2.4}$$

$$\frac{I_x}{I_c} = \frac{d_z^2}{d_c^2} \times \cos\beta, \tag{1.8.2.5}$$

where A_P is the pixel area, I_x is the intensity measured at the position of the pixel, I_c is the intensity measured at the centre of the camera, and the remaining distances and angles are shown in Figure 1.6.

The resulting geometry corrections to the intensity for each pixel, arising from Equation1.8.2.5, can be seen in Figure . add figure

The final illumination profile correction, combining both the laser profile and camera geometry, is shown in Figure . add figure The description used for this calibration is only an approximation to the lab set-up. The following factors cause deviations from this model:

- The pixels are not precisely aligned on the spherical focal surface; the pixel angle is fixed to its module's angle. The modules are aligned on the spherical focal surface.

- The light source is not point-like. It produces a diffuse emission, which likely reflects along the walls of the box.

A future study could further improve on the models used for the illumination correction.

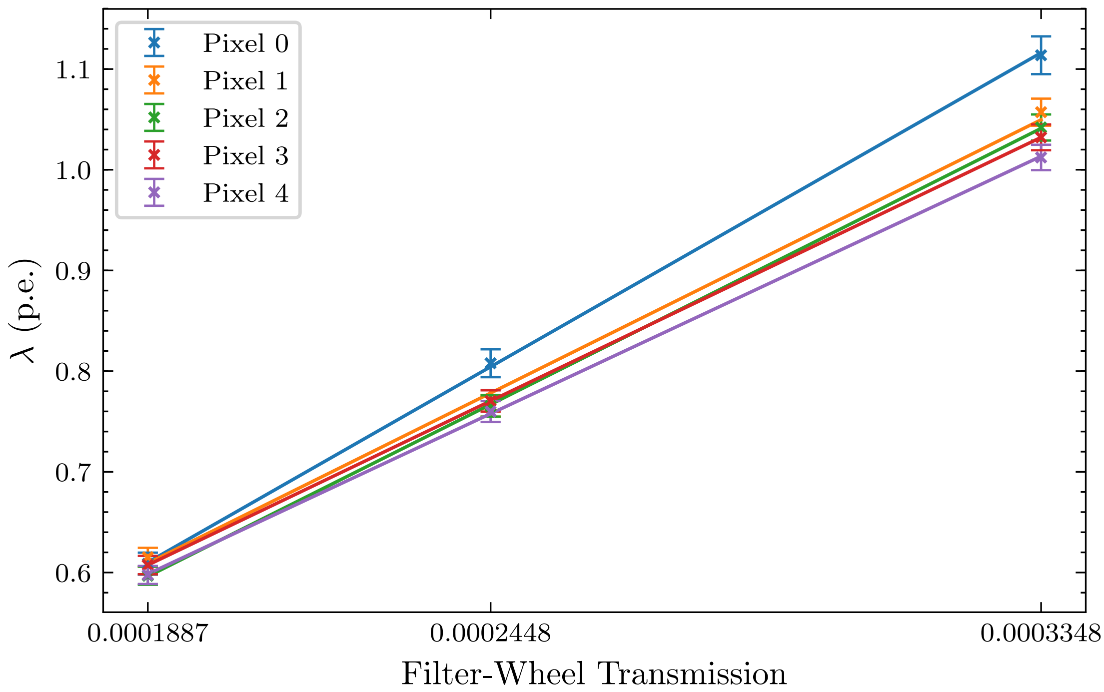

Figure 1.7: Example of the linear regression to obtain the relationship between filter-wheel transmission and average illumination in photoelectrons (λ), for 5 pixels. The values of λ are obtained from the simultaneous fits to the SPE spectra (Appendix **??**). The error bars on the points are the 1σ parabolic errors obtained from the covariance matrix of the fit)

1.8.3 Absolute Illumination

The method adopted to obtain a value for the absolute illumination was to use a fit to the SPE spectrum resulting from low-amplitude illumination of the pixels. Contained within this fit is the average illumination parameter, λ. The concept of the SPE fit is further covered in Chapter **??** and Appendix **??**.

By simultaneously fitting three illuminations, we obtained three values of λ per pixel. With the three filter-wheel transmissions (corresponding to the three illuminations) on the x-axis, these values of λ were linearly regressed (weighted by the 1σ parabolic error of the fit, σ_λ) to obtain the gradient M_λ and y-intercept C_λ per pixel. This linear regression is shown in Figure 1.7. The y-intercept represents the value of λ one would get with zero filter-wheel transmission, and therefore indicates the Night-Sky Background (NSB) and Dark-Count Rate (DCR). The variation in M_λ across the pixels arises from the folding of the illumination profile and the relative Photon Detection Efficiency (PDE). Therefore, the next step was to correct for the illumination profile contribution to the gradient. The resulting spread of M_λ is solely from the relative PDE (Figure). The calibration from filter-wheel

add figure, in this chapter or results chapter?

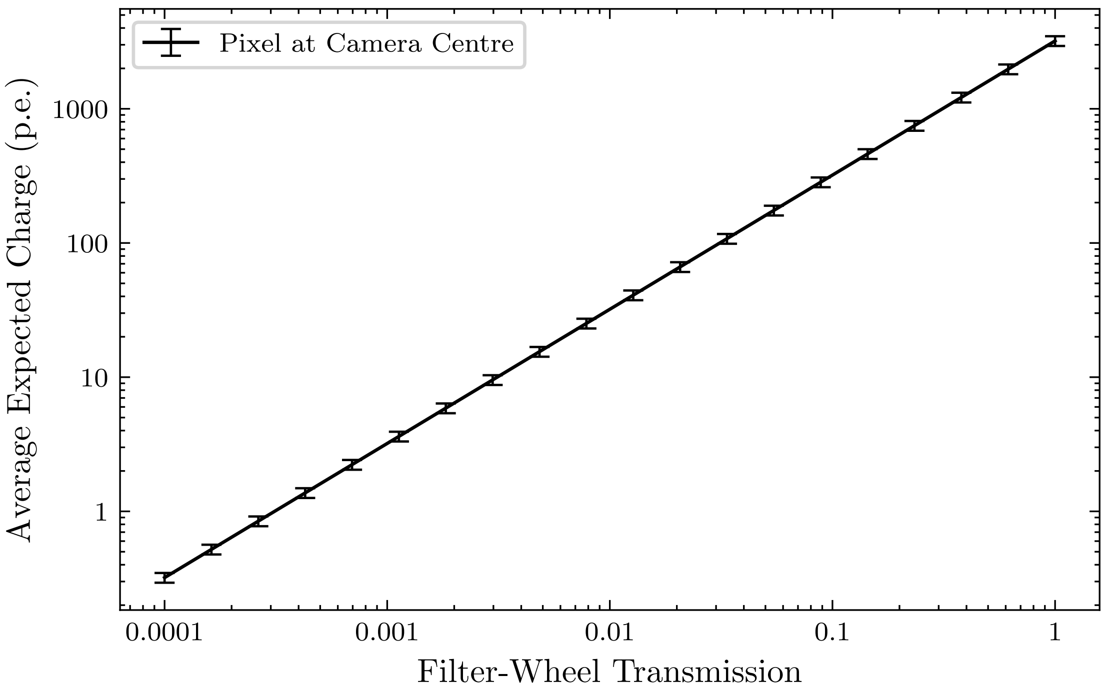

Figure 1.8: Relationship between filter-wheel transmission and average expected charge in photoelectrons resulting from the filter-wheel calibration. The black line shows the conversion for a theoretical pixel positioned exactly at the camera centre. The error bars are calculated from the weighted standard deviation of the gradient estimates between the pixels, explained in Section 1.8.5

transmission T_{FW} to the average illumination across the whole camera $\bar{I}_{pe}$ is then obtained by taking the averages of the linear regression coefficients:

$$\bar{I}_{pe} = \bar{M}_{\lambda} T_{\mathrm{FW}} + \bar{C}_{\lambda}, \tag{1.8.3.1}$$

1.8.4 Average Expected Charge

As we corrected for the NSB in the extracted signal value (Section **??**), the NSB contribution to Equation 1.8.3.1 ($\bar{C}_{\lambda}$) is subtracted to give us the charge we expect when illuminating the camera with a filter-wheel transmission T_{FW}, for a theoretical pixel perfectly positioned at the camera centre. This relation is shown in Figure 1.8. To obtain the average expected charge Q_{Exp} for each true camera pixel, this relation must be folded with the illumination profile correction factor F_{pix}:

$$Q_{\mathrm{Exp}} = \bar{M}_{\lambda} T_{\mathrm{FW}} F_{\mathrm{pix}}. \tag{1.8.4.1}$$

This expression is important for the flat-fielding calibration (Chapter **??**) and the calculation of the *Charge Resolution* for lab measurements (Chapter **??**), as it tells us for a certain pixel and filter-wheel transmission, what charge we should expect to measure on average.

1.8.5 Consideration of Errors and Uncertainty

When performing the weighted linear regression between λ_i and filter-wheel transmission T_{FW_i} (with weights $w_i = \frac{1}{\sigma^2_{\lambda_i}}$ accounting for the parabolic error in λ_i), the standard error on the estimate of the gradient per pixel, σ_{M_λ}, can be calculated with the relation derived by Taylor [2]:

$$\sigma_{M_\lambda} = \sqrt{\frac{\sum w_i}{\sum w_i \sum w_i T^2_{FW_i} - (\sum w_i T_{FW_i})^2}}, \quad i = 0, 1, 2, ..., N. \tag{1.8.5.1}$$

During the correction for the illumination profile on the gradient estimates, the illumination correction factors were also applied to the standard error on the gradient estimate.

While calculating the average gradient across the camera, $\bar{M}_\lambda$, the individual gradient estimates were weighted by their corresponding standard error. To calculate an uncertainty on the resulting value for $\bar{M}_\lambda$, the weighted standard deviation between the gradient estimates were also calculated. This uncertainty is illustrated in the error bars in Figure 1.8. The resulting conversion value from filter wheel transmission to expected charge for a theoretical pixel located at the centre of the camera was calculated to be $\bar{M}_\lambda = (3253.76 \pm 305.32)$ p.e.. check value

1.9 Readout Characteristics

define ADC

monitoring information

1.10 Nomenclature

charge/signal, waveform/trace, events

References

[1] A. Albert et al. “TARGET 5: A new multi-channel digitizer with triggering capabilities for gamma-ray atmospheric Cherenkov telescopes”. In: *Astroparticle Physics* 92 (2017), pp. 49–61. arXiv: 1607.02443. URL: http://linkinghub.elsevier.com/retrieve/pii/S0927650517301524.

[2] J. R. Taylor. *An introduction to error analysis : the study of uncertainties in physical measurements*. 2nd ed. Sausalito, Calif. : University Science Books, 1997, pp. 181–199.